Light Metals 2012 *Edited by: Carlos E. Suarez*
TMS (The Minerals, Metals & Materials Society), 2012

RESIDUAL STRESSES IN AS-CAST BILLETS: NEUTRON DIFFRACTION MEASUREMENT AND THERMOMECHANICAL MODELING

J.-M. Drezet[1], Th. Pirling[2] and C. Jaquerod[3]

[1]LSMX, Ecole Polytechnique Fédérale de Lausanne,
Station 12, CH-1015 Lausanne, Switzerland
jean-marie.drezet@epfl.ch
[2]Institut Laue Langevin, F-38042 Grenoble, France
[3] Constellium Valais SA, CH-3960 Sierre, Switzerland

Keywords: Extrusion billet, residual stresses, neutron diffraction, thermomechanical modeling

Abstract

Stress relief treatment is often required prior to sawing aluminum DC cast products in order to prevent crack formation and significant safety concerns due to the presence of high residual stresses generated during casting. Numerical models have been developed to compute these residual stresses and yet have only been validated against measured surface distortions. In the present contribution, the variation in residual strains and stresses have been measured using neutron diffraction in two AA6063 grain-refined cylindrical billet sections cast at two casting speeds. The measured residual stresses compare favorably with the numerical model, in particular the depth at which the axial and hoop stresses change sign. Such results provide insight into the development of residual stresses within castings and show that the stored elastic energy varies linearly with the casting speed, at least within the range of speeds that correspond to production conditions.

I Introduction

In the fabrication of aluminum extrusion products, the first step is the semi-continuous casting of a cylindrical billet. The most commonly used process is known as direct chill (DC) casting [1]. This process gives rise to large thermally induced strains that lead to several types of casting defects (distortions, cold cracks, porosity, solidification cracking, etc.). During casting, thermally induced stresses are partially relieved by permanent deformation. When these residual stresses overcome the deformation limit of the alloy, cracks are generated either during solidification (hot tears) or during cooling (cold cracks). The formation of these cracks usually results in rejection of the cast part. Furthermore, thermally induced deformations can cause downstream processing issues during the sawing stage prior to extrusion, when the billet is cut without thermal annealing between casting and sawing. For large diameter and high strength alloys, sawing becomes a delicate task owing to the risk of saw pinching or crack initiation ahead of the saw. Parts might be ejected and injure people or damage the equipment.

The computation of stresses during DC casting of aluminum alloys has been the scope of several studies since the late 90's [2-10] and is a well established technique nowadays. Many numerical models have allowed researchers to compute the ingot distortions and the associated residual stresses. The validation of these models was often done by comparing the computed and measured ingot distortions, e.g. the butt-curl [8] and the rolling face pull-in for rolling sheet ingots produced by DC [9] or electromagnetic casting [11].

Validation against the computed room-temperature residual stresses is limited simply owing to the difficulty of measuring the internal strains and the high variability in the measurements. While some measurements are available for quenching [12] or welding [13], they remain rare, uncertain and usually are limited to one or two components of the stress tensor, and to the skin of the billet for as-cast materials [14-15]. In contrast to destructive methods for measuring residual stresses (hole-drilling strain gage, cut compliance, layer removal technique), physical methods such as neutron, X-ray or ultra-sound diffraction are very attractive [16] since they can yield all stress components. In addition, the use of physical methods allows for measurements deep within a sample up to the energy limit of the beam. With the development of powerful neutron beams, it is now possible to measure the residual strains rather deep in light metal alloys such as aluminum and magnesium since these metals are relatively transparent to neutrons [17-18], as opposed to copper and iron. Such measurements allow for sophisticated model validation.

The FE model used to compute the stress build-up during casting is fully detailed in [18] together with the thermal and mechanical properties used for the AA6063 alloy. Using this model, the sawing itself was modeled by the removal of elements, similarly to the strategy adopted by Drezet et al. [19] to study possible crack initiation and propagation. Prior to this, the axisymmetric results from the casting simulation, above, are exported onto a 3D domain since the sawing process itself is not axisymmetric. Nevertheless, only half of the billet has to be modeled owing to the presence of a centre-line symmetry plane. It was shown that the movement of the saw induces a stress relaxation over a distance of 1.5 times the billet radius on both sides of the groove. The result is that, for residual stress measurements, the minimum billet section-length must be greater than at least three times the billet radius to ensure that the residual stresses at its mid-height are not relaxed during sawing. In the current context, this corresponds to a section-length of 48 cm.

Residual strain measurements have been undertaken on two AA6063 round billet sections 160 mm in radius (R), 0.6 m and 1 m in length and cast at 54 and 66 mm/min. The residual stress measurements have been carried out at the neutron diffractometer SALSA at ILL-Grenoble, France [20]. The goal of the present work is:

- to validate the residual stresses predicted by a finite element (FE) model of the DC casting process similar to the model previously developed by Drezet et al. [2],
- to compare the level of as-cast residual stresses in the steady state regime of casting for two different speeds,
- and to assess the influence of the casting speed on the elastic energy stored in the as-cast billet.

Section II provides a description of the material and the principles of residual stress measurement using neutron diffraction. The measurements are presented in section III for both casting speeds and compared with the values predicted by the FE model.

II. Material and residual stress measurement techniques

2.1 Material

The AA6063 alloy (Al Si 0.4 wt. % Mg 0.7 wt. %) is a heat treatable alloy. Its solidus, coherency (corresponding to a solid fraction of 65% for a grain refined structure) and liquidus temperatures are 557°C, 610°C and 655°C, respectively. These quantities were calculated using the software ProPHASE®, based on a model proposed by Sigli et al. [21]. The typical grain size in this casting was 100 +/- 30 microns with a globulitic microstructure. No texture was found owing to the use of grain refiner.

A 5.5 meter long extrusion billet, 320 mm in diameter, was cast semi-continuously at Constellium Valais SA, Switzerland. After the transient start-up phase, the casting speed was set to a minimum stable speed of 54 mm/min, for a cast length of 1 meter. Then the casting speed was increased to the maximum allowable speed over the next 1.5 m, keeping all other casting parameters, such as cooling conditions, constant. The rest of the billet was cast at 66 mm/min. The two billet sections, 60 cm and 1 m in length, were sawed from the two steady state casting regimes at 54 and 66 mm/min and transported to Institut Laue Langevin, Grenoble, for neutron diffraction residual stress measurements. The weight of the two billet sample was 130 kg for the 60 cm long section (66 mm/min) and 217 kg for 1 m long section (54 mm/min). M16 holes were drilled at both extremities for manipulation.

2.2. Neutron diffraction at Salsa

SALSA [20] is a neutron diffraction instrument designed for strain measurements through the accurate determination of lattice spacing. In a stressed material, the lattice spacing acts as a kind of strain gauge. The elastic strain is given by $\varepsilon = (d-d0)/d0$, where d0 and d are, respectively, the stress-free and actual lattice spacing for a given crystal plane family. Using Hooke's law, the measured strain can be converted to stress with the appropriate elastic constants. Diffraction can be understood in terms of the Bragg's law $\lambda = 2d\sin\theta$ where d is the lattice spacing, λ the wavelength and 2θ the diffraction angle. Therefore in order to measure the lattice spacing for determining strains and stresses, either the wavelength is fixed and the diffraction angle is measured (monochromatic angular dispersive) or the diffraction angle is fixed and the wavelength determined (polychromatic time-of-flight). In the case of monochromatic neutron source where only one diffraction peak is recorded, for fcc metals such as aluminum, the (311) diffracting planes are commonly used to measure the strain since they do not accumulate significant intergranular stresses and hence exhibit similar behavior as that of the bulk. The (311) is also recommended for use in the measurement of residual strains by neutrons in aluminum alloys by the ISO VAMAS standard [22]. A series of stress free reference samples, for measurement of the reference lattice constant d_0, were also acquired. These samples were electro-discharge machined along the billet radius every 20 mm in order to account for any variation in d_0 with position within the billet that may be present due to long range chemical inhomogeneities, i.e. macrosegregation. Located at ILL-Grenoble, SALSA uses a large crystal monochromator to select a particular neutron wavelength. The material to be studied is placed in this monochromatic neutron beam, and the scattered neutrons are collected on a large 2D detector to determine accurately the lattice spacing. The wavelength is constant (1.66 Å) and the position of the diffraction peak is recorded on a position sensitive detector. For the measurements at SALSA, 2 mm radial focusing collimators were used to reduce experimental errors introduced by the optics. A rather large instrumental gauge volume (2x2x15 mm^3), but with good lateral resolution in the scan direction, gave reasonable measurement times of on average 30 min.

2.3. Residual stress state in as-cast extrusion billets

In the DC casting of extrusion billets, the elastic stress/strain tensor has only four components due to the axisymmetric billet geometry and casting conditions. Furthermore, since the billet section used for the residual strain measurements was taken from a part corresponding to the steady-state regime of casting, it can be assumed that this tensor depends only on radial position. FE calculations [18, 23] have also shown that the fourth component of stress σ_{rz} is negligible thus further reducing the stress-strain tensor to three components, radial, hoop and axial. This tensor is therefore diagonal in the (r,θ,z) reference frame and can be described by Hooke's law, where E is Young's modulus (71.3 GPa) and ν the Poisson's ratio (0.3):

$$\sigma = \begin{pmatrix} \sigma_r \\ \sigma_\theta \\ \sigma_z \end{pmatrix} = \frac{E}{(1+\nu)(1-2\nu)} \begin{pmatrix} 1-\nu & \nu & \nu \\ \nu & 1-\nu & \nu \\ \nu & \nu & 1-\nu \end{pmatrix} \begin{pmatrix} \varepsilon_r \\ \varepsilon_\theta \\ \varepsilon_z \end{pmatrix} \quad (1)$$

For each of the three measured strain components, both the beam orientation and the position of the billet within the neutron chamber must be varied. For the radial component (cf. figure 1), the length of the beam path varies from almost zero at the billet surface to 2R at the billet centre. For the axial component (cf. figure 2), the beam path remains near $2\sqrt{2}\,R$ for each measurement location, whereas for the hoop component, the beam path increases from $\sqrt{2}\,R$ at the billet surface to 2R at the billet centre. Obviously, count times for the axial measurements are the longest. Figures 1 and 2 present the different billet positioning required measuring all three strain components.

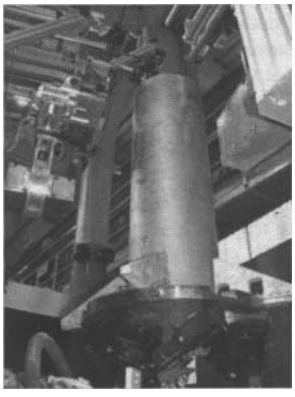

Figure 1: billet section positioning for measuring the radial and hoop strains at SALSA.

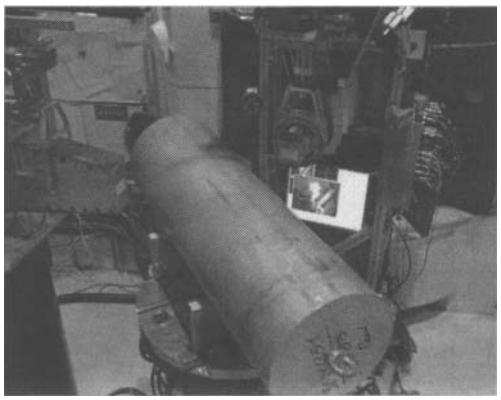

Figure 2: billet section positioning for measuring the axial strains at SALSA.

III. Results and discussion

3.1 Billet cast at 54 mm/min

Residual strains on the 1 m long AA6063 billet section cast at 54 mm/min were measured at the SALSA diffractometer. In total, roughly sixteen residual strain measurements were made along the radius of the billet in ~10 mm increments. The trace of the measured residual strains corresponds to the sum of the radial, hoop and axial elastic strains is presented in figure 3. To do so, a mean stress-free lattice parameter of 4.0504 Å for the (311) diffracting planes was used. The sum of the three as-cast elastic strain components computed using the FE model of DC casting [18] are also provided for comparison. The error bars are based on the scatter in the measurements, which is a function of the beam path-length within the billet. As can be seen in figure 3, it was possible to measure all three strain components over the entire radius of the billet. Indeed, the neutron beam was intense enough to measure the axial strain at the centre of the billet for which the beam path-length was longest, at 45 cm.

When the trace of the elastic strain tensor is positive, the material is in tension whereas when it is negative, it is in compression. This confirms our expectations; the centre of the billet is in tri-axial tension whereas its surface is in compression in the hoop and axial directions. Indeed the trace of the elastic strain tensor is proportional to the trace of the stress tensor:

$$\sigma_{kk} = \frac{E}{(1-2\nu)}\varepsilon_{kk} \qquad (2)$$

where an implicit summation of the repeated indices is assumed. In our case, the factor $E/(1-2\nu)$ is equal to 177 GPa.

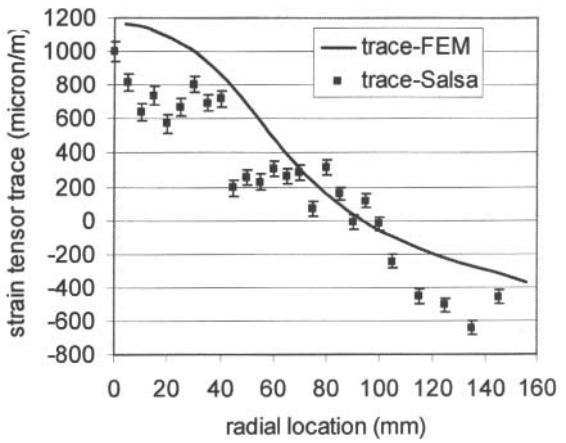

Figure 3: comparison between computed and measured traces of the elastic strain tensor for the billet section cast at 54 mm/min.

The radial distribution of the three stress components has been calculated at each radial position using Eq. 1. These stresses are shown in figures 4 to 6, along with the predicted stresses from the FE model. The error on strain measurement is reported on each of the points using the elastic constants. Again, the error becomes rather large for the axial stress. In a similar fashion to the residual strains, the centre of the billet is in tri-axial tension whereas its surface is in compression in the hoop and axial directions as already reported by Hannart et al. [3] and Fjaer and Mo [4]. This residual stress state develops because of the fast surface cooling rates applied during the casting process which efficiently cools the surface of the billet. The cold shell then hinders the contraction of the hot core region, leading to large interior tensile stresses. This effect is known as "skin-core effect" [25]. Furthermore, the agreement between the measured stress components and the FE predictions is very good for the radial and hoop components and weaker for the axial component especially at the billet centre where FE results underestimate the stress level.

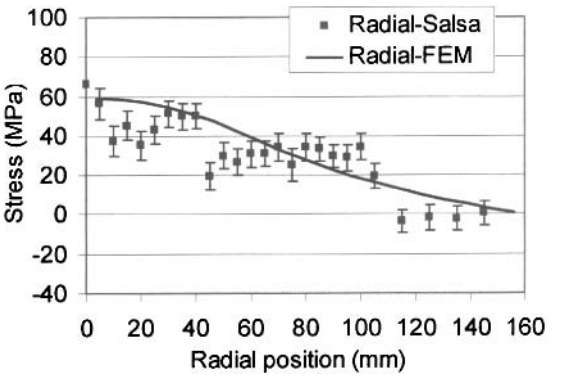

Figure 4: comparison between computed and measured radial stress component within the billet cast at 54 mm/min

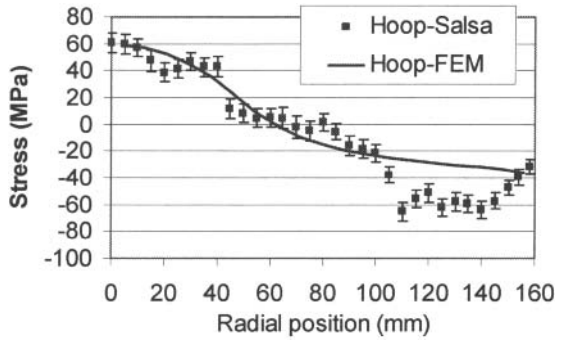

Figure 5: comparisons between computed and measured hoop stress component within the billet cast at 54 mm/min

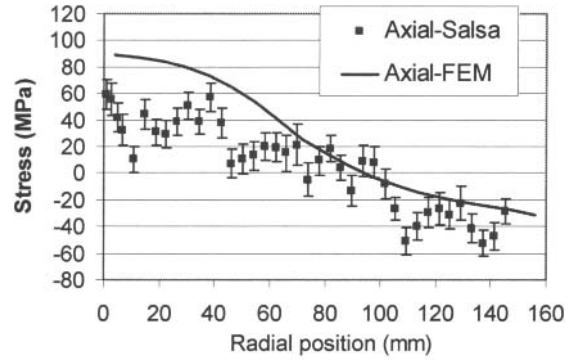

Figure 6: comparisons between computed and measured axial stress component within the billet cast at 54 mm/min

The locations where the axial and hoop stress components change sign are also very close to the measured ones. Note also that the measured radial stress component at the billet surface is 2.5 MPa whereas it should be zero. This gives us an idea of the precision that can be obtained with such neutron measurements.

3.2 Billet cast at 66 mm/min

Residual strains on the 0.6 m long AA6063 billet section cast at 66 mm/min were measured at the neutron diffractometer SALSA. As measuring time was rather low owing to a high neutron flux, roughly thirty two residual strain measurements were made along the radius of the billet in ~5 mm increments. Furthermore, a mean stress-free lattice parameter of 4.0504 Å was used as no substantial variation along the radius was found.

The radial distribution of the three stress components has been calculated at each radial position using Eq. 1. These stresses are shown in figures 7 to 9, along with the predicted stresses from the FE model. The statistical error is larger for the axial stress at the billet centre owing to a longer beam path length, but still below 10 MPa. As for the billet cast at 54 mm/min, the centre of the billet is in tri-axial tension whereas its surface is in compression in the hoop and axial directions. Again, the agreement between the stress components measured at SALSA and the FE predictions is very good for all three components. The FE results always fall within the measured values except near the billet surface for the hoop stress and at the billet centre for the axial stress. The locations where the axial and hoop stress components change sign are also very close to the measured ones. Note also that the measured radial stress component close to the billet surface, in reality 4 mm under the surface, is 4 MPa and tend to zero when approaching the billet surface in spite of possible small texture and grain size effect at the very surface.

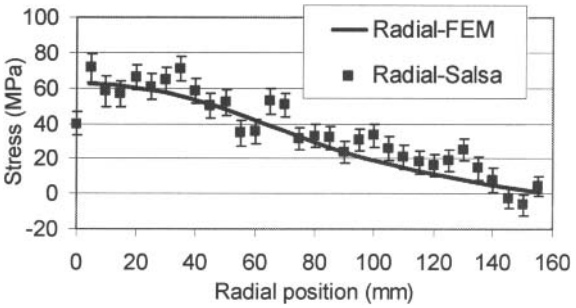

Figure 7: comparison between computed (FEM) and measured radial stress component within the billet cast at 66 mm/min.

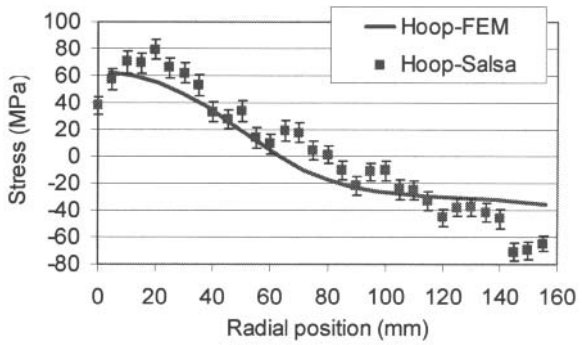

Figure 8: comparison between computed (FEM) and measured hoop stress component within the billet cast at 66 mm/min.

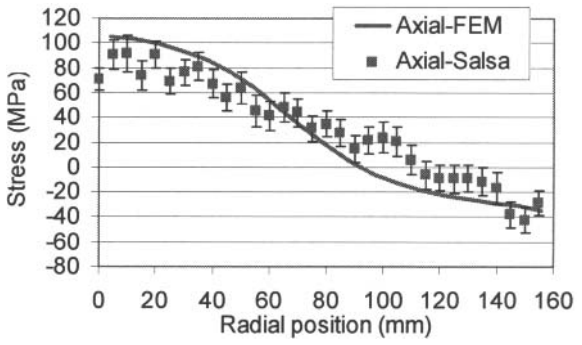

Figure 9: comparison between computed (FEM) and measured axial stress component within the billet cast at 66 mm/min.

A good indication of the validity of the neutron diffraction measurements is the value of radial and hoop stress components at the zero radial position. Indeed, at the billet centre-line and for symmetry reasons, both radial and hoop stresses and strains are equal in materials with Poisson's ratio lower than 0.5. This is the case at 54 mm/min (cf. figures 4 and 5) and at 66 mm/min (cf.

figures 7 and 8) where measured axial and hoop stresses are identical at the billet centre.

The overall agreement between FE results and measured values induces confidence in the numerical model. As the casting speed increases, the stress level both in compression at the billet surface and in tension in the interior increases slightly. Nevertheless, the FE model underestimates the level of compression (hoop stress) at the billet surface. This can be attributed to a poor description of the cooling conditions along the billet surface during casting. Besides, kinematic hardening is not taken into account although stresses change sign from tension to compression at the very billet surface during casting [1]. In addition, possible precipitation of stable or metastable phases might occur during the cooling of the solid metal and could explain the stress plateaus observed at the low casting speed in figures 4 to 6. These plateaus disappear at the high casting speed owing to higher cooling rates. Transmission electron microscopy (TEM) and small angle X-ray scattering (SAXS) are to be carried out at different distances from the billet centerline in order to determine the nature and size of these precipitates.

3.3 Stored elastic energy

The stored elastic energy in a billet section of length H and radius R is given by:

$$W = \frac{1}{2}\int_V \sigma:\varepsilon \, dV = 2\pi H \int_0^R \frac{\sigma_r\varepsilon_r+\sigma_\theta\varepsilon_\theta+\sigma_z\varepsilon_z}{2} \, rdr \qquad (3)$$

As the FE results fall within the measured values (cf. figures 4-6 for the low casting speed and figures 7-9 for the high casting speed), the stored energy can be calculated using the FE predictions. The radial distribution of the elastic energy density is shown in figure 10 for the two casting speeds. Increasing the casting speed leads to an increase in the elastic energy density especially from the centre of the billet up to half of its radius.

Calculating integral (3) for our two billet samples (R = 160 mm) yields an elastic energy of W/H per unit length and a density of elastic energy per unit volume D = $W/(\pi R^2 H)$. The results are summarized in table 1. The level of stored elastic energy is larger than the level found after quenching of 6xxx aluminum thick plates [25]. This can be explained by the fact that thermally induced deformations and associated stress build up are of the same nature in casting and in quenching although the composition of the alloy has a great influence and temperatures are much higher in casting compared to quenching.

Casting speed Vcast	Elastic energy per unit length (W/H)	Elastic energy per unit volume D	D/Vcast
mm/min	kJ/m	kJ/m3	kJ.min/mm.m3
54	0.975	12.1	0.2241
66	1.2	14.8	0.2242

Table 1: linear and volumetric elastic energies as a function of the casting speed.

As the casting speed increases, the stored elastic energy per unit length or volume increases. The higher this value, the higher is the risk to get erratic dissipation of energy during casting (solidification or cold cracking) or when sawing the as-cast billet [19]. Casting recipes should be adapted in order to keep this value at an acceptable level.

It is interesting to notice in Table 1 that the ratio of the stored elastic energy to the casting speed is constant. In other words, the stored energy density is proportional to the casting speed at least within the range of speeds investigated here. This is explained by the fact that during casting, the depth of the liquid pool that forms within the billet is also proportional to the casting speed. The deeper the sump depth is, the greater are the thermally induced deformations and associated stresses and thus the higher is the stored elastic energy as shown in figure 10.

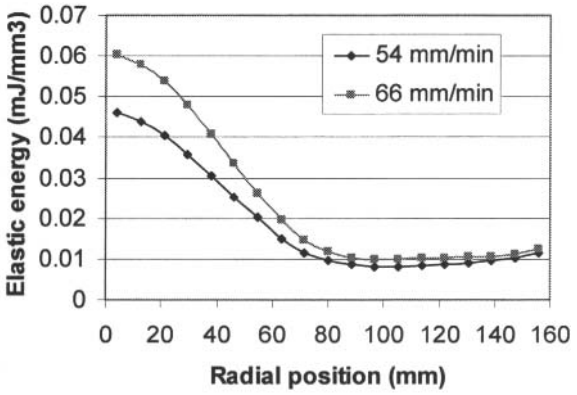

Figure 10: radial distribution of the stored elastic energy density for two casting speeds.

Conclusion

The as-cast residual stresses have been measured on steady-state sections of an AA6063 extrusion billet cast at two different casting speeds in order to generate different residual stress profiles. Neutron diffraction measurements have been carried out at SALSA, ILL-Grenoble, France. All measured results agree relatively well with the computed values of a FE model of DC casting considering the numerous input parameters entering into the model (alloy properties, cooling conditions, etc.). In particular, the locations where axial and hoop stresses change sign are well predicted by the model. Still, the FE model underestimates the level of compression (hoop stress) at the billet surface. This can be attributed to a poor description of the cooling conditions along the billet surface during casting and to the absence of kinematic hardening in the mechanical description. Finally, it is shown that the stored elastic energy within the as-cast billet varies linearly with the casting speed, at least within the range of investigated speeds that correspond to production conditions. Further analysis of possible phase precipitation taking place during casting is still under progress.

Acknowledgements

The authors express their deep acknowledgements to Constellium Valais SA for providing the two billet sections on which neutron diffraction measurements and to the international Neutron Source at ILL for the provision of beam time.

References

1. J.-M. Drezet *"Direct Chill and Electromagnetic Casting of Aluminium Alloys: Thermomechanical Effects and Solidification Aspects"*, PhD work no. 1509, EPF-Lausanne, July 1996. http://library.epfl.ch/en/theses/
2. J.-M. Drezet, M. Rappaz, *Modelling of Ingot Distortions during Direct Chill Casting of Aluminium Alloys* , Met. Mat. Trans. A, 27A, 1996, pp. 3214-3225.
3. B. Hannart, F. Cialti, R. V. Schalkwijk, *Thermal Stresses in DC Casting of Aluminum Slabs: Application of a Finite Element Model*, Light Metals 1994, A. T. Tabereaux Ed., TMS, 1994, pp. 879-887.
4. H. Fjaer and A. Mo: *Alspen: a mathematical model for thermal stresses in direct chill casting of aluminium billets*, Met. Mat. Trans. A, 21B, 1990, pp. 1049-1061.
5. J. Sengupta, S.L. Cockcroft, D.M. Maijer, A. Larouche, *Quantification of temperature, stress, and strain fields during the start up phase of DC casting process by using a 3D fully coupled thermal and stress model for AA5182 ingots*, Mat. Sc. Eng A, 397, 2005, pp. 157-177.
6. W. Boender, A. Burghardht, E. P. van Klaveren, J, Rabenberg, *Numerical Simulation of DC casting, Interpreting the results of a Thermo-Mechanical Model*, Light Metals 2004, A. T. Tabereaux Ed., TMS, 2004, pp. 679-684.
7. O. Ludwig, J.-M. Drezet, B. Commet, B. Heinrich, *Modelling of Internal Stresses in DC casting and Sawing of High Strength Aluminum Alloys slabs* , in Modeling of Casting Welding and Advanced Solidification Processes, Eds. C.-A. Gandin and M. Bellet, pp. 185-192, Nice, 2006.
8. W. Droste, J.-M Drezet, G.-U Gruen and W. Schneider: *3D Modeling of Ingot Geometry Development of DC-cast Aluminium Ingots during the Start-up Phase*, in Continuous Casting, Eds: K. Ehrke and W. Schneider, DGM, Wiley-VCH, Frankfurt 2000, pp. 175-183.
9. W. Droste, G.-U Grün, W. Schneider and J.-M. Drezet : *Thermo-Mechanical Modeling to Predict Shrinkage, Shape and Mold Openings for DC-Cast Rolling Ingots*, in Light Metals, Eds. Wolfgang Schneider, TMS 2002, Seattle, pp. 703-708.
10. A.B. Phillion, D. Maijer and S.L. Cockcroft: *Coupled Thermal-Stress Model of the Start-up Phase of the Aluminum Direct Chill Casting Process: Predictions Relating to Hot Tearing* in Model Casting, Welding & Adv Solidif Proces XI, TMS, (2006), 807-814.
11. J. W. Evans: *The use of electromagnetic casting for Al. alloys and other metals*, Journal of metals, TMS, May 1995, pp. 38-41.
12. K. Escobar et al.: *On the residual stress control in aluminium alloys 7050*, Materials Science Forum vols. 396-402 (2002), p. 1235-1240.
13. S. Ganguly, M. E. Fitzpatrick and L. Edwards: *Comparative neutron and synchrotron X-rax diffraction studies to determine residuals stress on an as-welded AA2024 plate*, Materials Science Forum vols. 790-491 (2005), pp. 223-228.
14. J. Moriceau: *Thermal stresses in continuous DC casting of Al alloys, discussion of hot tearing mechanisms*, Light Metals (TMS), 1975, p. 119-133
15. S. A. Levy et al.: *Residual stress measurements for studying ingot cracking*, Light Metals (TMS), 1974, p. 571-585.
16. J. Lu, *Handbook of Measurement of residual stresses*, Society for Experimental Mechanics, Inc. The Fairmont Press, Ed. J. Lu, 1996.
17. H. Hao, D.M. Maijer, M.A. Wells, S.L. Cockcroft and R.B. Rogge, *Prediction and measurement of residual stresses/strains in a direct chill casting magnesium alloy billet* in Magnesium Technology, (2005), 223-228.
18. J.-M. Drezet and A. Phillion: *As-cast residual stresses in an aluminum alloy AA6063 billet: neutron diffraction measurements and finite element modeling*, in Met. and Mat. Trans. Vol. 41 A, pp. 3396-3404, December 2010.
19. J.-M. Drezet, O. Ludwig, C. Jaquerod and E. Waz: *Fracture prediction during sawing of DC cast high strength aluminium alloy rolling slabs* in Inter. Journal of Cast Metals, 2007, vol. 20, no. 3, p. 163-170.
20. Strain imager for engineering applications SALSA, Institut Laue Langevin, Grenoble, France http://www.ill.eu/instruments-support/instruments-groups/instruments/salsa/
21. C. Sigli, L. Maenner, C. Sztur and R. Shahani, *Phase diagram, solidification and heat treatment of aluminium alloys*, Proc. International Conference on Aluminum Alloys, T. Sato, S. Kumai, T. Kobayashi and Y. Murakami Eds, JILM, 1998, pp.87-98.
22. G.A. Webster: VAMAS TWA 20 standard, ISO Technical report, 2001
23. J.-M. Drezet, A. Evans, C. Jaquerod and A. Phillion: *Measurement of as-cast residual stresses in an aluminium alloy AA6063 billet using neutron diffraction*, Jim Evans Honorary Symposium, Eds. B. Li, B. Thomas, L. Zhang, F.-M. Doyle and A. Campbell, TMS, 2010, pp. 43-52.
24. J.-M. Drezet and M. Rappaz, *Ingot Distortions and Residual Stresses in Direct Chill Casting of Aluminium Alloys* in Proceedings of the 4th European Conference on Residual Stresses, ECRS 1996, SF2M, Eds. S. Denis et al., Cluny, France, pp. 357-366.
25. F. Heymès, B. Commet, B. Dubost, P. Lassince, P. Lequeu and G.M. Raynaud, *Development of new Al Alloys for distortion free machined aluminum aircraft components*, 1st International Non-ferrous Processing and Technology Conference, St Louis, Missouri, 10-12 March 1997